

Aging dynamics in the polymer glass of poly(2-chlorostyrene): Dielectric susceptibility and volume

Koji Fukao* and Daisuke Tahara

Department of Physics, Ritsumeikan University, Noji-Higashi 1-1-1, Kusatsu 525-8577, Japan

(Received 26 April 2009; revised manuscript received 21 August 2009; published 10 November 2009)

Aging dynamics was investigated in the glassy states of poly(2-chlorostyrene) by measuring the complex electrical capacitance during aging below the glass transition temperature. The variations with time and temperature of the ac dielectric susceptibility and volume could be determined by simply measuring the variation in the complex electrical capacitance. Isothermal aging at a given temperature for several hours after an intermittent stop in constant-rate cooling is stored in the deviations of both the real and imaginary parts of the complex ac dielectric susceptibility and volume. During cooling after isothermal aging, the deviation of the ac dielectric susceptibility from the reference value decreases and almost vanishes at room temperature. By contrast, the deviation in volume induced during isothermal aging remains almost constant during cooling. The simultaneous measurement of ac dielectric susceptibility and volume clearly revealed that the ac dielectric susceptibility exhibits a full rejuvenation effect, whereas the volume does not show any rejuvenation effects. We discuss a plausible model that can reproduce the present experimental results.

DOI: [10.1103/PhysRevE.80.051802](https://doi.org/10.1103/PhysRevE.80.051802)

PACS number(s): 71.55.Jv, 81.05.Lg, 77.22.Ch

I. INTRODUCTION

It is well known that below the glass transition temperature, the dynamical mode called the α process is totally frozen [1]. This frozen state is referred to as the glassy state. In polymeric systems, segmental motion is the microscopic origin of the α process [2]. However, even in the glassy state, there is a very slow change in the structure and dynamics when approaching a real equilibrium state. This phenomenon is known as aging or physical aging [3]. Several interesting phenomena, including memory effects and rejuvenation, occur during physical aging [3–5]. These effects, which are related to aging processes, are frequently observed in many disordered systems, including polymer glasses [6–11], spin glasses [12–15], and other disordered systems [16–18]. Therefore, we expect that a common physics lies behind aging phenomena. The elucidation of this common physics is the ultimate goal in this field.

In previous papers [8,9], we measured the complex dielectric susceptibility as a function of the aging time for various thermal histories, including isothermal aging at a given aging temperature below the glass transition temperature T_g , the constant-rate mode, and the temperature cycling mode for the glassy states of poly(methyl methacrylate) (PMMA). For isothermal aging, both the real and imaginary parts of dielectric susceptibility decrease with increasing aging time. Because the dielectric susceptibility originating from the orientational polarization of electric dipoles can be regarded as a measure of disorder, the reduction in the dielectric susceptibility implies that the glassy state is approaching a more stable equilibrium state.

We also investigated the glassy dynamics for thin films of polystyrene (PS) by measuring the aging time dependence of the complex electrical capacitance $C^*(\equiv C' - iC'')$ for isothermal aging at a given temperature [19,20]. The capacitance

measurements clearly revealed that the imaginary part of the complex electrical capacitance C'' decreases with increasing aging time, while the real part of the complex electrical capacitance C' increases with increasing aging time. If the effect of temperature on the geometrical capacitance is neglected, the temperature (and time) dependence of the dielectric susceptibility will be the same as that of the electrical capacitance. The observed results for C'' suggest that the aging time dependence of C'' for PS is consistent with that observed for PMMA.

By contrast, the aging time dependence of C' for PS appears to be totally different from that of the real part of the dielectric susceptibility for PMMA. In a previous paper [20], we discussed the aging time dependence of not only the dielectric susceptibility but also the geometrical capacitance and we were able to reproduce the observed aging time dependence of C' over a wide frequency range. According to this interpretation, the increase in C' is associated with a reduction in the volume (i.e., an increase in the density), while the decrease in the imaginary part is associated with a decrease in the ac dielectric susceptibility. In other words, measuring the complex electrical capacitance enables us to simultaneously measure both the volume and the imaginary part of the ac dielectric susceptibility under exactly the same conditions. However, because the polarity of PS is very small, it was difficult to obtain sufficiently strong signal of the dielectric loss and we were unable to fully confirm the validity of our interpretation in our previous paper [20].

In this paper, we used poly(2-chlorostyrene) (P2CS) as a model system for complex capacitance measurements using dielectric relaxation spectroscopy. The structure of P2CS is quite similar to that of PS, with the exception that a chlorine atom Cl is attached to the benzene ring. The presence of the chlorine atom in the chain enhances the polarity of this polymeric system and hence P2CS can be regarded as an ideal system for dielectric measurements. We performed capacitance measurements on thin films of P2CS under a variety of thermal conditions in order to investigate the glassy dynam-

*Corresponding author; fukao.koji@gmail.com

ics of this polymeric system. Through such measurements, we attempted to elucidate the nature of unusual behavior, such as memory and rejuvenation effects, observed during aging in the glassy state.

In this paper, the experimental details are described in Sec. II, the results observed during isothermal aging are given in Sec. III A, and measurements of the Kovacs effect are described in Sec. III B. The observed results relating to memory and rejuvenation effects are given in Sec. III C and then a possible scenario for such effects is proposed in Sec. III D. We have also measured the thickness dependence of aging phenomena and glass transition dynamics; these results will be published in the near future.

II. EXPERIMENTAL

Polymer samples used in this study are P2CS purchased from Polymer Source, Inc. (weight-averaged molecular weight $M_w=3.3 \times 10^5$, $M_w/M_n=2.2$). Using spin coating, we prepared thin films of P2CS from a toluene solution on a glass substrate on which aluminum (Al) had been vacuum deposited. The film thickness was controlled by varying the concentration of the solution; in this study, we used a film thickness of 22 nm. After annealing at 343 K under vacuum for 2 days to remove solvents, Al was again vacuum deposited to serve as an upper electrode. In order to obtain reproducible results, several heating cycles up to and exceeding the bulk value of the glass transition temperature T_g were carried out before capacitance measurements were performed on the relaxed as-spun films. The value of T_g in the thin films with $d=22$ nm was 383 K. The thickness was evaluated before measurements from the value of the electrical capacitance at 273 K for the as-prepared films in the manner previously reported [21,22].

Capacitance measurements were carried out using an LCR meter (Agilent Technology, 4284A and E4980A) for the frequency f range from 20 Hz to 1 MHz during cooling and heating between 423 and 273 K at a rate of 1 K/min as well as during isothermal aging at various aging temperatures T_a ($=300$ – 357 K). The complex electrical capacitance of the sample condenser C^* was measured as a function of temperature T and aging time t .

In this paper, we employed the following two temperature protocols:

(1) *Isothermal aging*. In this temperature protocol, the temperature changes from a high temperature 413 K (above T_g) to an aging temperature T_a (below T_g) and then the temperature is maintained at T_a for t_a hours. We denote this protocol as $\mathcal{I}(T_a, t_a)$.

(2) *Constant-rate mode*. The temperature is decreased from 413 to 273 K at a constant rate of 1 K/min and then it is increased from 273 to 413 K at the same rate. This is a simple constant-rate mode and we refer to this temperature change as the reference mode. In addition to the above thermal treatment, we included an intermittent stop at T_a for t_a hours during cooling from 413 to 273 K. We denote this temperature protocol as $\mathcal{C}(T_a, t_a)$. According to this notation, the reference mode corresponds to the protocol $\mathcal{C}(T_a, 0)$ for any value of T_a .

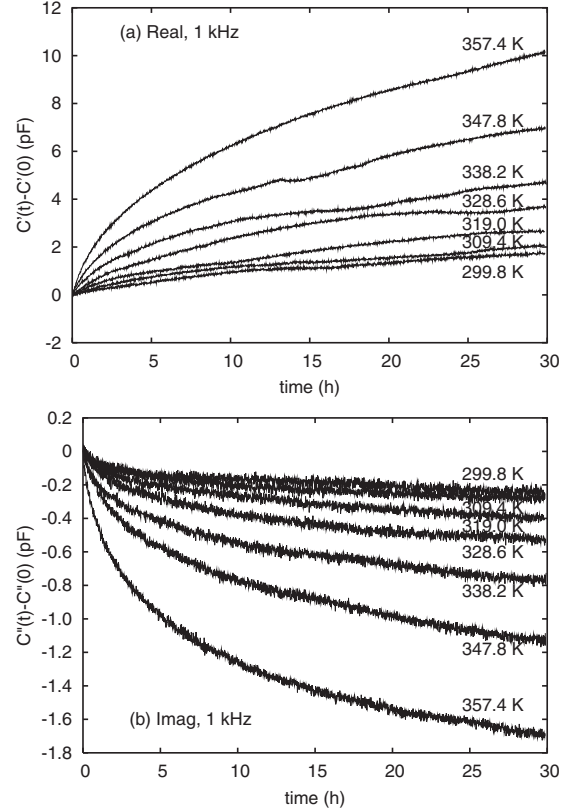


FIG. 1. Aging time dependences of the deviation of (a) the real part and (b) the imaginary part of the complex electrical capacitance from the value at the initial time $t=0$ in P2CS thin films with $d=22$ nm for various aging temperatures $T_a=357.4$, 347.8, 338.2, 328.6, 319.0, 309.4, and 299.8 K. The applied electric field has a frequency f of 1 kHz.

III. RESULTS AND DISCUSSION

A. Isothermal aging

Figure 1 shows the aging time dependences of the real and imaginary parts of the electrical capacitance C' and C'' for thin films of P2CS during isothermal aging $\mathcal{I}(T_a, t_a)$, where T_a lies between 299.8 and 357.4 K, and $t_a=30$ h. The deviations of C' and C'' from their values when the temperature first reaches the isothermal aging temperature T_a are plotted. Figure 1 shows that C' increases with aging time during isothermal aging, while C'' decreases with aging time. The aging time dependences of C' and C'' for thin films of P2CS are qualitatively the same as those observed in PS films in a previous study by us [20]. Because of the higher polarity of P2CS, we were able to obtain much clearer time dependences of C' and C'' for P2CS than for PS. Here, we consider the physical origin of the observed aging time dependences of C' and C'' for the polymeric system P2CS.

The origin of the variation in the electrical capacitance can be attributed to the change in the volume or density and the change in the ac dielectric susceptibility during aging. Each component of the complex electrical capacitance C^* can be written as follows:

$$C'(f, T, t) = [\epsilon_{zz}(T, t) + \epsilon'_{\text{disp}}(f, T, t)]C_0(T, t), \quad (1)$$

TABLE I. Relative change in C' and C'' during isothermal aging at 357.4 K for $\Delta t=30$ h for the thin films of P2CS with thickness of 22 nm. The upper part is for C' and the lower part is for C'' .

$f(\text{Hz})$	20 Hz	100 Hz	1 kHz	10 kHz	100 kHz
C' (pF)	9201.0	9148.7	9098.9	9066.5	9000.9
$\Delta C'$ (pF)	3.6	7.0	10.1	11.7	13.3
$\frac{1}{C'} \frac{\Delta C'}{\Delta t}$ (h^{-1})	1.3×10^{-5}	2.6×10^{-5}	3.7×10^{-5}	4.3×10^{-5}	4.9×10^{-5}
C'' (pF)	77.6	47.4	35.5	85.6	–
$\Delta C''$ (pF)	5.1	3.2	1.7	1.3	–
$\frac{1}{C''} \frac{\Delta C''}{\Delta t}$ (h^{-1})	2.2×10^{-3}	2.3×10^{-3}	1.5×10^{-3}	0.5×10^{-3}	–

$$C''(f, T, t) = \epsilon''_{\text{disp}}(f, T, t) C_0(T, t), \quad (2)$$

where ϵ'_{disp} and ϵ''_{disp} are the components of dielectric constants due to molecular motion and consequently they are strongly dependent on the frequency of the applied electric field for the temperature range in which molecular motion can be observed. The parameter ϵ_∞ is the dielectric constant for a very high-frequency range where there is no contribution from molecular motion and C_0 is the geometrical capacitance that can be evaluated from the size of the condenser prepared from the thin polymer films using the relation $C_0 = \epsilon_0 \frac{S}{d}$. Here, S is the area of the electrode, d is the thickness of the sample, and ϵ_0 is the dielectric permittivity in vacuum. To evaluate C_0 , we use the thickness d at 273 K and $S=8 \times 10^{-6} \text{ m}^2$.

During isothermal aging, we anticipate that the density will increase with aging time ($\frac{\partial d}{\partial t} < 0$ for aging); this is usually referred to as densification of polymeric materials [23]. By contrast, the ac susceptibility (i.e., the magnetic and dielectric susceptibilities) decreases with increasing aging time for polymer glass and spin glass [8,9,12,13]. This is well understood since the dielectric constant, for example, can be regarded as a measure of the disorder with respect to the orientation of the dipole moments.

As for the volume change, the effective area of the electrode S remains constant under the present measurement conditions. In this case, the volume change can be described by the thickness change $\frac{\partial d}{\partial t}$ and we obtain the following relations:

$$\frac{1}{C_0} \frac{\partial C_0}{\partial t} \approx - \frac{1}{d} \frac{\partial d}{\partial t}, \quad \frac{1}{\epsilon_\infty} \frac{\partial \epsilon_\infty}{\partial t} = - \frac{1}{d} \frac{\partial d}{\partial t}. \quad (3)$$

Here, it should be noted that ϵ_∞ is related to the density of the material ρ via the Clausius-Mossotti equation [24] and hence the change in ϵ_∞ with time or temperature includes contributions from the change in density. Performing a simple calculation, we obtain the following relations:

$$\frac{1}{C'} \frac{\partial C'}{\partial t} = \frac{2\epsilon_\infty + \epsilon'_{\text{disp}}}{\epsilon_\infty + \epsilon'_{\text{disp}}} \left[- \frac{1}{d} \frac{\partial d}{\partial t} + \zeta(f) \frac{1}{\epsilon'_{\text{disp}}} \frac{\partial \epsilon'_{\text{disp}}}{\partial t} \right], \quad (4)$$

$$\frac{1}{C''} \frac{\partial C''}{\partial t} = - \frac{1}{d} \frac{\partial d}{\partial t} + \frac{1}{\epsilon''_{\text{disp}}} \frac{\partial \epsilon''_{\text{disp}}}{\partial t}, \quad (5)$$

where

$$\zeta(f) = \frac{\epsilon'_{\text{disp}}(f)}{2\epsilon_\infty + \epsilon'_{\text{disp}}(f)}.$$

Equation (5) clearly shows that the time derivative of C'' is controlled by simple competition between the change in the thickness and the change in the ac dielectric susceptibility ϵ''_{disp} . In the case of PS, dilatometric measurement shows that the initial specific volume of PS, v_0 , is $0.972 \text{ cm}^3/\text{g}$ and the amount of the decrease in specific volume Δv is $0.0025 \text{ cm}^3/\text{g}$ for the isothermal aging at $86.1 \text{ }^\circ\text{C}$ for $\Delta t = 30 \text{ h}$ [23]. Therefore, we obtain the relation $|\frac{1}{v_0} \frac{\Delta v}{\Delta t}| = 8.6 \times 10^{-5} \text{ h}^{-1}$ and hence $|\frac{1}{d} \frac{\partial d}{\partial t}| = 2.9 \times 10^{-5} \text{ h}^{-1}$ for the aging at $86.1 \text{ }^\circ\text{C}$. As for the electric capacitance, the relative change in C'' during isothermal aging can be evaluated from the present measurement on thin films of P2CS as listed in Table I. Therefore, for low frequencies below 1 kHz, the following relation holds: $|\frac{1}{d} \frac{\partial d}{\partial t}| / |\frac{1}{C''} \frac{\partial C''}{\partial t}| < 0.02$.

On the other hand, the time derivative of C' includes a frequency-dependent factor $\zeta(f)$ as Eq. (4) shows. In order to evaluate the value of $\zeta(f)$, we can use the values of ϵ'_{disp} and ϵ_∞ for various frequencies listed in Table II. It is found that ζ is a decreasing function of f and that $\zeta = 8.8 \times 10^{-3}$ for 10 Hz and $\zeta = 5.8 \times 10^{-4}$ for 10 kHz. Although ζ is much smaller than 1 even at 10 Hz, the value ζ becomes still smaller as f increases. Therefore, it is concluded that $\zeta \ll 1$ for the frequency range $f > 10 \text{ Hz}$. Furthermore, as shown in Table I, the increasing rate of C' for aging at 357.4 K for 30 h is

TABLE II. Frequency dependence of ϵ' , ϵ'_{disp} , and $\zeta(f)$ for thin films of P2CS with thickness of 995 nm [27]. $\epsilon_\infty = 2.7583$ for $f = 100 \text{ kHz}$. ϵ'_{disp} can be evaluated from the relation $\epsilon'_{\text{disp}} = \epsilon' - \epsilon_\infty$.

f	10 Hz	100 Hz	1 kHz	10 kHz
ϵ'	2.8072	2.7814	2.7686	2.7615
ϵ'_{disp}	0.0489	0.0231	0.0103	0.0032
$\zeta(f)$	8.8×10^{-3}	4.2×10^{-3}	1.9×10^{-3}	5.8×10^{-4}

$$\frac{1}{C'} \frac{\Delta C'}{\Delta t} = 4.9 \times 10^{-5} \text{ h}^{-1} \quad \text{for } 100 \text{ kHz.} \quad (6)$$

If the relation $\zeta \ll 1$ is valid and $\zeta \frac{1}{\epsilon'_{\text{disp}}} \frac{\partial \epsilon'_{\text{disp}}}{\partial t}$ can be neglected, we expect the following relation from Eq. (4):

$$\frac{1}{C'} \frac{\partial C'}{\partial t} \approx -2 \frac{1}{d} \frac{\partial d}{\partial t}. \quad (7)$$

As shown above, $\frac{1}{d} \frac{\partial d}{\partial t} = 2.9 \times 10^{-5} \text{ h}^{-1}$ for PS. Here, we expect that the same relation is valid also for P2CS. On this assumption, we obtain the relation

$$\frac{1}{C'} \frac{\partial C'}{\partial t} \approx 5.8 \times 10^{-5} \text{ h}^{-1}. \quad (8)$$

Comparing Eq. (6) and (8), the agreement between the two values is not perfect, but good enough for us to judge that Eq. (7) is valid at frequencies above 100 kHz. As a result, in the case of P2CS, the contribution from the thickness change is much larger than that from the change in the ac dielectric susceptibility for the real part of the electrical capacitance C' at 100 kHz. As f decreases, $\frac{1}{C'} \frac{\partial C'}{\partial t}$ becomes smaller and $\zeta(f)$ becomes larger. Therefore, we expect that the contribution from ϵ'_{disp} will become larger than that from d at low frequencies even for the real part of the electrical capacitance C' .

On the basis of the above considerations, it is concluded that the increase in C' and the decrease in C'' with increasing aging time observed for $f=1$ kHz in Fig. 1 are mainly associated with the reduction in the volume and the reduction in the ac dielectric susceptibility, respectively. In the following section, we show further evidence for the hypothesis that the change in C' is associated with the volume change.

B. Kovacs effect

Kovacs *et al.* performed an interesting experiment that demonstrated the existence of memory effects in polymer glasses [4]. In their experiments, volume relaxation was measured at a point in the glassy state located on a line extrapolated from the equilibrium line in the liquid state. Because this point lies on the equilibrium line, no further volume changes are expected at that point. However, their results revealed that the volume relaxation strongly depends on the thermal history of the polymer before reaching the equilibrium point. In other words, the thermal history can be stored within the glassy state of polymers. In the present study, as shown in Sec. III A, the increase in C' is mainly associated with the change in the volume or thickness at high frequencies. In this case, because C' is approximately inversely proportional to d , the value $1/C'$ should have the same temperature dependence as the volume under the present conditions.

Figure 2(a) shows the temperature dependence of the inverse of C' , which can be regarded as the volume in this case, for various thermal histories. The sample is cooled from 413 K ($>T_g$) at which the sample is thermally equilibrated down to T_a . The sample is isothermally aged at $T_a = 347.8$ and 357.6 K for 80 and 40 h, respectively. The sample is then heated again to $T_f = 367.1$ K, which is located on the line extrapolated from the equilibrium line above T_g

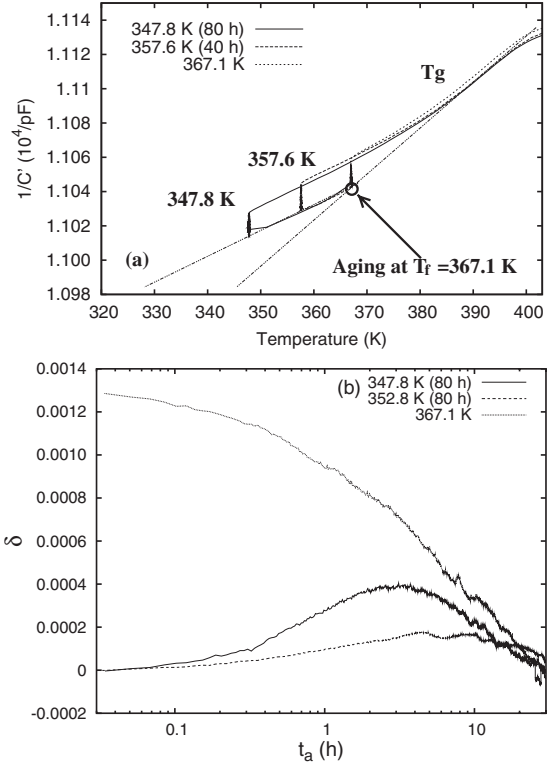


FIG. 2. (a) Temperature dependence of $1/C'$ for $f=10$ kHz for three different thermal treatments. From $T_0=413$ K to $T_f=367.1$ K (1) broken curves: via isothermal aging at $T_a=357.6$ K for $t_a=40$ h, (2) solid curve: via isothermal aging at $T_a=347.8$ K for $t_a=80$ h, (3) dotted curves: direct. (b) The relative change in the volume or C'^{-1} as a function of the logarithm of the aging time after isothermal aging at $T_f=367.1$ K.

and the temperature is maintained at T_f . Here, the volume of the sample is expected not to change with time at T_f because the sample has already attained an equilibrium volume at T_f .

However, contrary to our expectation, the value of $1/C'$ exhibits an interesting aging time dependence during isothermal aging at T_f as shown in Fig. 2(b). Figure 2(b) shows the relative deviation of the volume δ as a function of aging time during isothermal aging at $T_f=367.1$ K after two different thermal histories (indicated by the solid and broken curves). Here, δ is defined as

$$\delta(t) = \frac{v(t) - v(0)}{v(0)} = \frac{C'^{-1}(t) - C'^{-1}(0)}{C'^{-1}(0)}, \quad (9)$$

where $v(t)$ and $C'^{-1}(t)$ are the volume and the inverse of C' at time t . In Fig. 2(b), the aging time dependence of $\delta(t)$ is also shown for isothermal aging at T_f after direct quenching from 413 K to T_f (indicated by the dotted curve). Figure 2(b) shows that δ increases with increasing aging time and then decreases back to its initial value after going through a maximum. Furthermore, the time at which $1/C'$ shows a maximum is strongly dependent on the aging temperature T_a before the sample reaches the temperature T_f . This suggests that polymer glass can store memories related to its previous thermal history even after it is heated to the temperature T_f . Because the value $1/C'$ is proportional to the volume of the

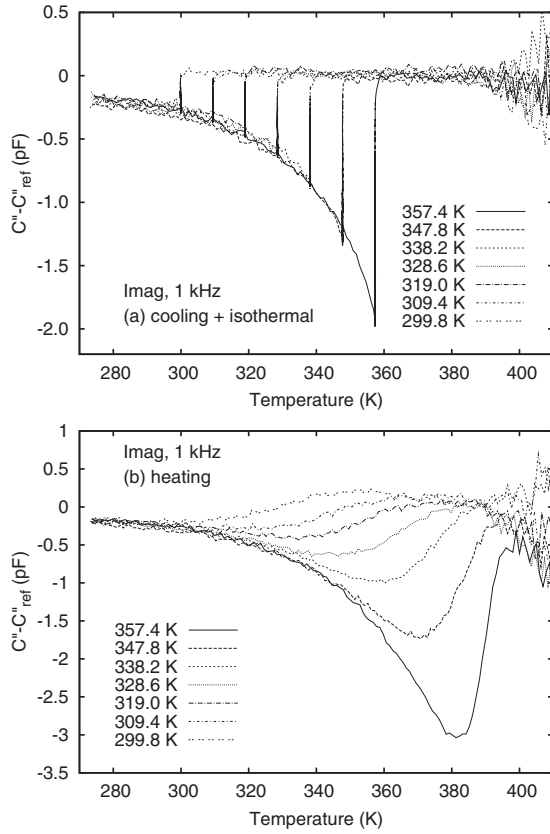


FIG. 3. Temperature dependence of the deviation of the imaginary part of electrical capacitance from the reference values observed (a) during cooling including isothermal aging at various aging temperatures T_a for 30 h and (b) the subsequent heating cycle. The cooling rate is 1.0 K/min. The reference values are observed during cooling at the same rate without any isothermal aging.

polymeric system, the present measurements can well reproduce the well-known Kovacs experiments [4]. Therefore, we regard this result as strong experimental evidence for the validity of our interpretation that, in this case, $1/C'$ has the same temperature and time dependence as the volume of this polymeric system. As a result, it is possible to simultaneously measure the volume and the ac dielectric susceptibility by performing a single measurement of the electrical capacitance of P2CS.

C. Memory and rejuvenation effects for C'

For P2CS thin films, we have performed capacitance measurements for constant-rate mode, in which we have observed memory and rejuvenation effects for other polymeric systems such as poly(methyl methacrylate) [8,9]. As mentioned in the previous sections, for P2CS, we simultaneously observed the variations of both the ac dielectric susceptibility and volume with time and temperature changes. Therefore, we can extract the aging behavior not only of the ac dielectric susceptibility but also of the volume of exactly the same polymeric glasses by conducting a single capacitance measurement.

Figure 3 shows the temperature dependence of the deviation of C'' from the reference value C''_{ref} , $\Delta C'' (\equiv C'' - C''_{\text{ref}})$,

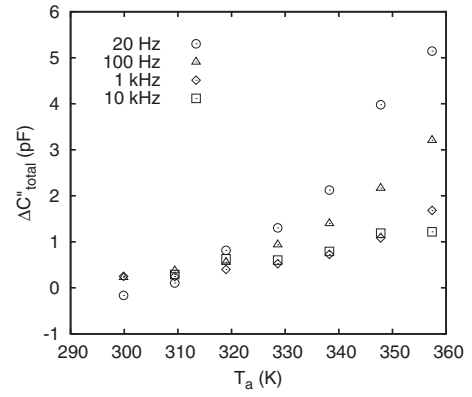


FIG. 4. The dependence of the relaxation strength $\Delta C''_{\text{total}}$ on the isothermal aging temperature at various frequencies for thin films of P2CS.

during the constant-rate mode $\mathcal{C}(T_a, t_a)$, where $T_a = 357.4 - 299.8$ K and $t_a = 30$ h. Here, the reference value C''_{ref} is defined as follows. We perform capacitance measurements during simple heating and cooling at the rate of 1 K/min and then we obtain the reference value C''_{ref} at any temperature for heating and cooling, separately. The results observed for cooling and heating are shown in Figs. 3(a) and 3(b), respectively. Figure 3(a) shows that during cooling from a high temperature in the liquid state, $\Delta C''$ remains at zero because the liquid state is an equilibrium state. Then, for isothermal aging at T_a , $\Delta C''$ decreases from zero due to aging; this moves the system toward an equilibrium state. However, as the temperature decreases again from T_a to room temperature, the deviation induced during isothermal aging decreases with decreasing temperature. At 273 K, the deviation almost vanishes, that is, the polymer glass is *fully rejuvenated* as far as the ac dielectric susceptibility ϵ''_{ac} is concerned. During the subsequent heating, $\Delta C''$ decreases again with increasing temperature as if the polymer glass knew the path along which it was cooled during the preceding cooling cycle and $\Delta C''$ increases after going through a minimum at T'_a , which is about 30 K above the isothermal aging temperature T_a . The results observed in the constant-rate mode for thin films of P2CS clearly demonstrate that there are memory and rejuvenation effects, similar to those observed in PMMA [6,8].

These results were observed for P2CS at $f = 1$ kHz. We also measured the frequency dependence of $\Delta C''$ as a function of temperature for the constant-rate mode. It is found that the temperature dependence of $\Delta C''$ is qualitatively independent of frequency and only the relaxation strength of $\Delta C''$ depends on the frequency and the aging temperature. Figure 4 shows the aging temperature dependence of the relaxation strength $\Delta C''_{\text{total}}$ of $\Delta C''$ as a function of the frequency of the applied electric field. Here, we define $\Delta C''_{\text{total}}$ as $\Delta C''_{\text{total}} \equiv \Delta C''(0) - \Delta C''(t_a)$, where $t_a = 30$ h. Figure 4 shows that $\Delta C''_{\text{total}}$ increases with decreasing frequency at a given aging temperature and that it increases with increasing temperature at a given frequency. The value of $\Delta C''_{\text{total}}$ for isothermal aging at 357.4 K for $f = 20$ Hz is about 5 times greater than that for $f = 10$ kHz and hence $\Delta C''_{\text{total}}$ also increases with increasing aging temperature and with decreasing frequency. Therefore, this dependence of $\Delta C''_{\text{total}}$ on T_a

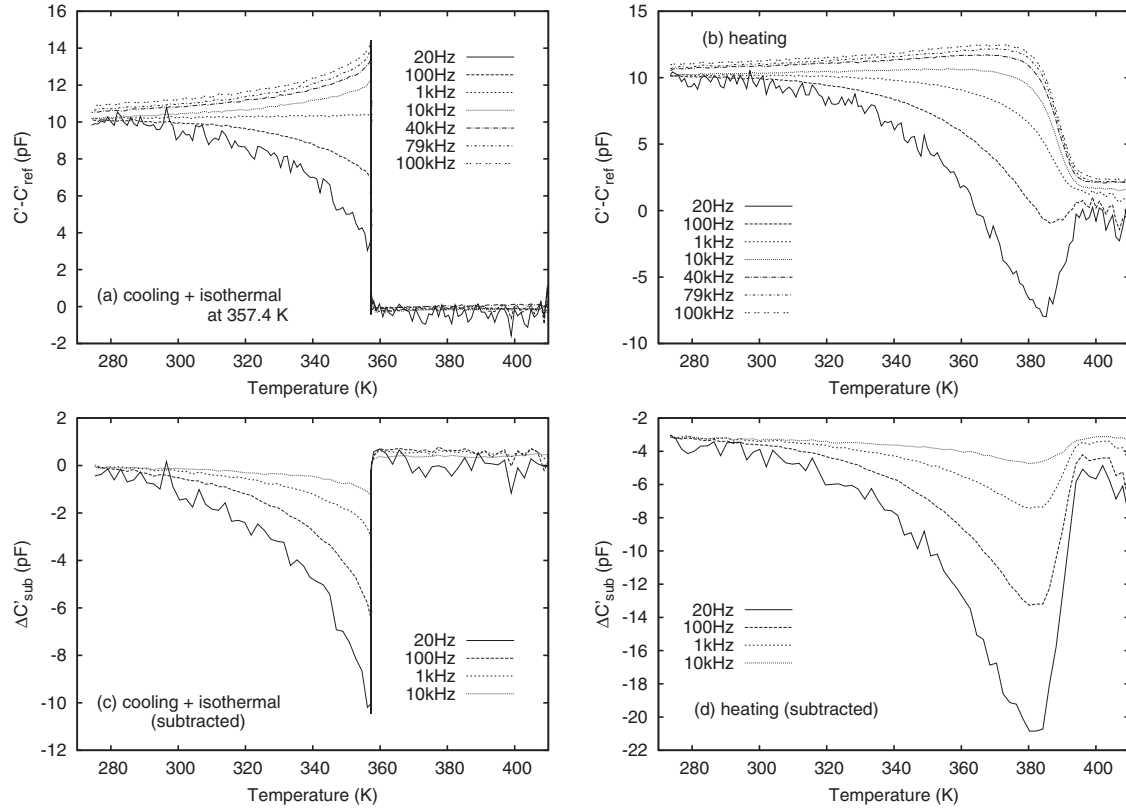


FIG. 5. Temperature dependence of the deviation of C' from the reference value C'_{ref} for various frequencies between 20 Hz and 100 kHz (a) during cooling including isothermal aging at 357.4 K and (b) during the subsequent heating cycle. The lower figures show the temperature dependence of $\Delta C'$ after subtracting $\Delta C'$ at 10 kHz, $\Delta C'_{\text{sub}}$, for various frequencies between 20 Hz and 10 kHz (c) during cooling including isothermal aging at 357.4 K and (d) during the subsequent heating cycle.

and f suggests that the main driving force that induces the change during isothermal aging is the mobility due to the lower frequency tail of the α process. The observed frequency dependence of $\Delta C'_{\text{total}}$ for P2CS is the same as that observed for PMMA by several groups [6,8]. These results were observed for the imaginary part of the complex electrical capacitance in the case of thin films of P2CS. We now consider the results for the real part of the electrical capacitance C' .

Figure 5 shows the temperature dependence of C' for the frequency range between 20 Hz and 100 kHz observed for the constant-rate mode ($T_a=357.4$ K, $t_a=30$ h), which is exactly the same temperature protocol as that used for C'' as shown in Fig. 3. Here, the deviation of C' from the reference value, $\Delta C' (\equiv C' - C'_{\text{ref}})$, is plotted as a function of temperature. Figure 5(a) shows that $\Delta C'$ at 100 kHz increases with increasing aging time during isothermal aging at $T_a=357.4$ K. This is consistent with the results shown in Fig. 1(a). Furthermore, during cooling after isothermal aging, $\Delta C'$ decreases slightly with decreasing temperature, but most of the deviation induced during isothermal aging is still present at 273 K. For frequencies above 40 kHz, there is only very weak frequency dependence as can be seen in Fig. 5. For higher frequencies, the change in $\Delta C'$ is mainly associated with the change in volume because the contribution from the ac dielectric susceptibility is appreciable only at low frequencies for the temperature range investigated in this study. Therefore, this result suggests that the volume de-

creases with increasing aging time during isothermal aging at T_a . The volume change induced during isothermal aging still survives even at 273 K. This means that the volume change *does not show full rejuvenation*. Here, it should be noted that during cooling after isothermal aging, $\Delta C'$ decreases slightly and then approaches a finite constant value. This does not imply that the volume increases with decreasing temperature, only that the deviation of the volume from the reference value increases with decreasing temperature. Thus, the volume change is not unphysical.

During the subsequent heating cycle, $\Delta C'$ remains almost constant up to about 380 K ($>T_a=357.4$ K) and it then decreases rapidly to zero as shown in Fig. 5(b). This suggests that the volume also retains the *memory* of the temperature at which isothermal aging was performed.

When the frequency is reduced from 40 kHz to 20 Hz, the temperature change in $\Delta C'$ strongly depends on frequency both for cooling and heating as shown in Figs. 5(a) and 5(b). The relaxation strength of $\Delta C'$ induced during isothermal aging at T_a decreases with decreasing frequency. As we have already discussed in Sec. III A, this strong frequency dependence may be due to the frequency dispersion of the ac dielectric susceptibility induced by molecular motion. Therefore, we expect that $\Delta C'$ will show the same temperature dependence after subtracting the contribution from the change in volume. For this purpose, we evaluated the value of $\Delta C'_{\text{sub}}(T, f)$ using the following relation:

$$\Delta C'_{\text{sub}}(T, f) \equiv \Delta C'(T, f) - \Delta C'(T, 100 \text{ kHz}). \quad (10)$$

Figures 5(c) and 5(d) show $\Delta C'_{\text{sub}}$ for both cooling and heating in constant-rate mode. In this figure, $\Delta C'_{\text{sub}}$ corresponds to the real part of the ac dielectric susceptibility ϵ'_{disp} . Therefore, Figs. 5(c) and 5(d) show that ϵ'_{disp} exhibits *full rejuvenation and memory effects* for the constant-rate mode in a very similar way as that observed for C'' , that is, ϵ''_{disp} , although volume does not show full rejuvenation. The present capacitance measurements revealed that there is a distinct difference in the aging behaviors of the volume and the complex ac dielectric susceptibility.

D. Model for aging dynamics

In the previous sections, we successfully observed memory and rejuvenation effects for the ac dielectric susceptibility and volume by measuring the capacitance. As a result, we found that the ac dielectric susceptibility reveals that the relaxation strength due to isothermal aging has a clear dependence on the aging temperature and the frequency of the electric field and that the susceptibility shows full rejuvenation and memory effects, while the volume does not exhibit full rejuvenation. Here, we interpret the memory and rejuvenation effects in the light of the observed results.

We adopt the following assumptions. The aging dynamics is controlled by the α process, which occurs at low frequencies at a given temperature in the glassy state. The temperature dependence of the characteristic time of the α process $\tau_\alpha(T)$ is usually given by the Vogel-Fulcher-Tammann law (VFT law) $\tau_\alpha(T) = \tau_0 \exp(U/(T - T_V))$ [25], where τ_0 , U , and T_V are constants. The relaxation time of the α process has a broad distribution [26]. The mean value is equal to $\tau_\alpha(T)$ and the distribution of the characteristic frequency ω of the α process at temperature T is given by $g(\omega, T)$. We also assume that $g(\omega, T)$ has a single peak shape with a finite width. The peak position ω_α approximately corresponds to $1/\tau_\alpha$. Hence, we obtain the relation

$$\frac{1}{\tau_\alpha(T)} \sim \omega_\alpha(T) = \langle \omega \rangle = \int_{\omega=0}^{\omega=\infty} \omega g(\omega, T) d(\log_e \omega).$$

1. Debye relaxation

During aging, each mode of the α process with relaxation rate ω can independently contribute to the change in dynamics and structure. Each mode with relaxation rate ω can contribute to the overall dielectric relaxation as a Debye relaxation process with the corresponding single relaxation time ($\sim 1/\omega$) and hence the complex dielectric constant $\epsilon_D^*(\omega_E, \omega)$ for the mode with the relaxation rate ω can be described as

$$\epsilon_D^*(\omega_E, \omega) = \frac{\Delta \epsilon}{1 + i \frac{\omega_E}{\omega}} \equiv \Delta \epsilon \cdot \tilde{\epsilon}_D^*(\omega_E, \omega), \quad (11)$$

where $\omega_E (\equiv 2\pi f)$ is the angular frequency of the applied electric field and $\Delta \epsilon$ is the dielectric relaxation strength. From Eq. (11), we obtain the real and imaginary parts of $\tilde{\epsilon}_D^*(\omega_E, \omega) (\equiv \tilde{\epsilon}'_D - i\tilde{\epsilon}''_D)$ as follows:

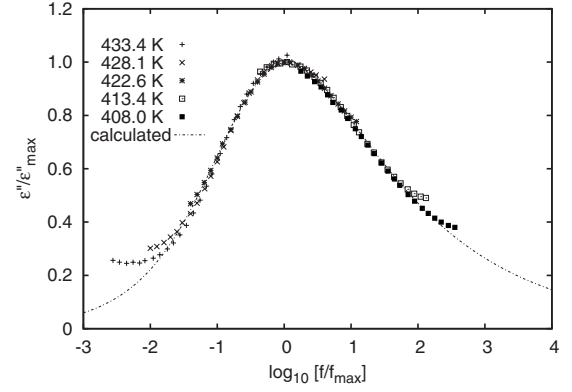


FIG. 6. Dependence of the normalized dielectric loss on the normalized frequency for thin films of P2CS with thickness of 22 nm for various temperatures between 408.0 and 433.4 K. The set of the data ($f_{\text{max}}, \epsilon''_{\text{max}}$) gives us the location of the dielectric loss peak of the α process at a given temperature. Dotted curve is reproduced using the HN equation with the best-fitting parameters $\Delta \epsilon_{\text{HN}} = 5.54$, $\alpha_{\text{HN}} = 0.606$, $\beta_{\text{HN}} = 0.430$, and $\tau_0 = 0.530$.

$$\tilde{\epsilon}'_D(\omega_E, \omega) = \frac{1}{1 + \left(\frac{\omega_E}{\omega}\right)^2}, \quad (12)$$

$$\tilde{\epsilon}''_D(\omega_E, \omega) = \frac{\frac{\omega_E}{\omega}}{1 + \left(\frac{\omega_E}{\omega}\right)^2}. \quad (13)$$

The loss curve given by Eq. (13) has a characteristic width, the full width at the half maximum (FWHM) amounting to 1.14 decades. As for the real part $\tilde{\epsilon}'_D$, there is a crossover region where the value of $\tilde{\epsilon}'_D$ changes from 1 to 0 with increasing frequency ω_E . The characteristic width of this crossover region is 1.14 decade, which is the same value as that for the width of the loss curve $\tilde{\epsilon}''_D$.

2. Distribution of the relaxation rate

On the other hand, the distribution function of the relaxation rate ω of the α process has a much broader width than that of the Debye relaxation process. Figure 6 shows the dielectric loss ϵ'' normalized with respect to the peak value ϵ''_{max} as a function of frequency f normalized with peak frequency f_{max} for thin films of P2CS with thickness of 22 nm for various temperatures between 408.0 and 433.4 K [27]. The dotted curve is calculated using the Havriliak-Negami (HN) equation [28]

$$\epsilon^* = \frac{\Delta \epsilon_{\text{HN}}}{[1 + (i\omega_E \tau_0)^{\alpha_{\text{HN}}}]^{\beta_{\text{HN}}}}, \quad (14)$$

where $\Delta \epsilon_{\text{HN}}$ is the dielectric relaxation strength, τ_0 is the relaxation time, α_{HN} is the parameter for the distribution of relaxation times, and β_{HN} is the parameter for the asymmetry of the dielectric loss profile. The best-fitting parameters are as follows: $\Delta \epsilon_{\text{HN}} = 5.54 \pm 0.04$, $\alpha_{\text{HN}} = 0.606 \pm 0.008$, $\beta_{\text{HN}} = 0.430 \pm 0.015$, and $\tau_0 = 0.530 \pm 0.03$. On the basis of the

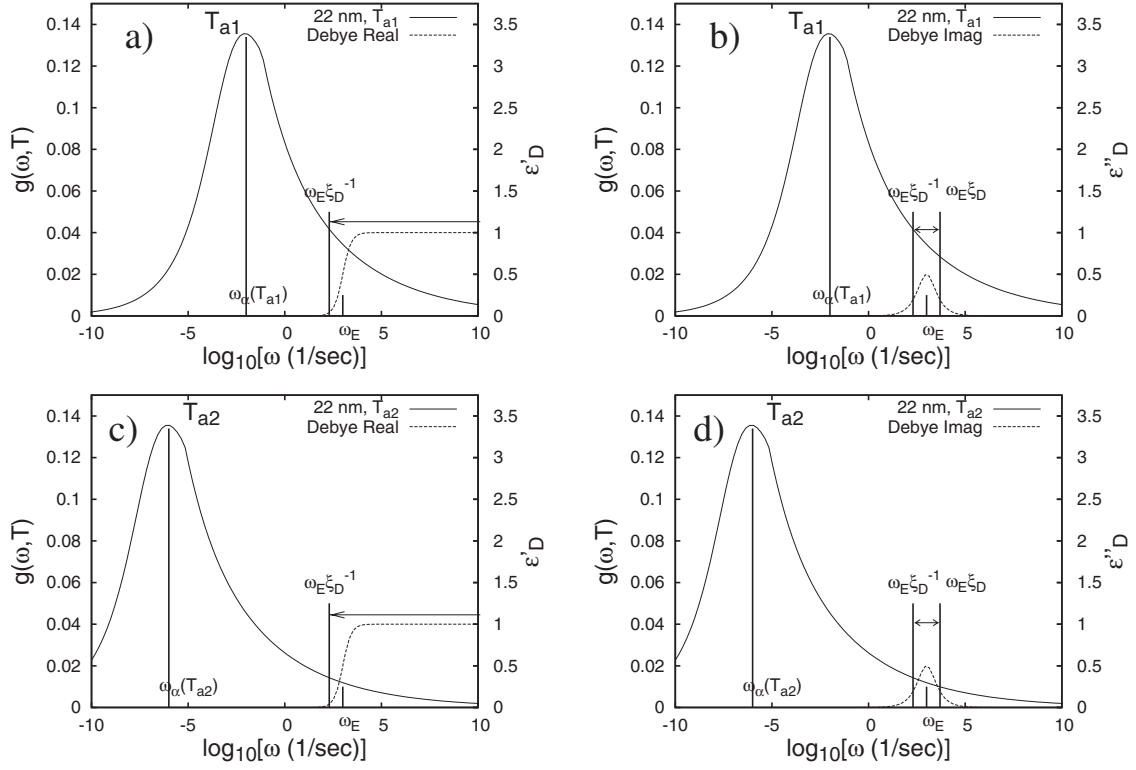


FIG. 7. Dependence of the distribution function of the relaxation rate $g(\omega, T)$ (solid curve) and the real and imaginary parts of dielectric constant ϵ'_D and ϵ''_D (dotted curve) for two different temperatures T_{a1} and T_{a2} ($T_{a1} > T_{a2}$). (a) $g(\omega, T_{a1})$ and ϵ'_D , (b) $g(\omega, T_{a1})$ and ϵ''_D , (c) $g(\omega, T_{a2})$ and ϵ'_D , and (d) $g(\omega, T_{a2})$ and ϵ''_D . Here, T_{a1} and T_{a2} are chosen so that $\log_{10} \omega_\alpha(T_{a1})$ and $\log_{10} \omega_\alpha(T_{a2})$ are located at -2.3 and -6.1 , respectively. The curves of $g(\omega, T)$ are calculated using Eqs. (15) and (16) with best-fitting parameters given in the caption of Fig. 6.

HN equation, the distribution function of the relaxation time τ , $F(s)$, can be calculated analytically as follows:

$$F(s) = \frac{1}{\pi} [1 + 2e^{\alpha_{\text{HN}}(x_0 - s)} \cos \pi \alpha_{\text{HN}} + e^{2\alpha_{\text{HN}}(x_0 - s)}]^{-\beta_{\text{HN}}/2} \times \sin \left[\beta_{\text{HN}} \tan^{-1} \left(\frac{e^{\alpha_{\text{HN}}(x_0 - s)} \sin \pi \alpha_{\text{HN}}}{1 + e^{\alpha_{\text{HN}}(x_0 - s)} \cos \pi \alpha_{\text{HN}}} \right) \right], \quad (15)$$

where $s = \log_e \tau$ and $x_0 = \log_e \tau_0$ [22]. Using this function $F(s)$, we can obtain the distribution function of the relaxation rate ω , $g(\omega, T)$ as follows:

$$g(\omega, T) = F(-\log_e \omega). \quad (16)$$

In the case of thin films of P2CS with thickness of 22 nm, the distribution function of the relaxation rate of the α process could successfully be evaluated using Eqs. (15) and (16) with the parameters for the HN equation as shown by the solid curves in Fig. 7. Although the solid curves in Fig. 7 include an arbitrary shift along the horizontal axis depending on the temperature T , their shape is unambiguously determined by Eq. (15). The FWHM of the distribution peak is about 6 decades, which is much larger than that of the loss peak due to the Debye relaxation.

In the case of a broad distribution of the relaxation rates of the α process, the observed complex dielectric constant $\epsilon^*(\omega_E, T)$ can be described as a sum of the contributions from all single Debye relaxations

$$\epsilon^*(\omega_E, T) = \int_0^\infty \epsilon_D^*(\omega_E, \omega) g(\omega, T) d(\log_e \omega) \quad (17)$$

$$= \Delta \epsilon \int_0^\infty \frac{1}{1 + i \frac{\omega_E}{\omega}} g(\omega, T) d(\log_e \omega). \quad (18)$$

3. Aging of ac dielectric susceptibility

During aging, the dielectric constant shows a decrease with increasing aging time t_a . The origin of the decrease in the dielectric constant at a given frequency during aging is mainly due to the shift of the tail of the α process to the lower frequency side [29]. In this case, $\omega_\alpha(T)$ decreases with increasing t_a and as a result, the peak position of $g(\omega, T)$ is shifted along the ω axis as a function of t_a . Here, after adding the additional variable t_a to ϵ^* and g , we can rewrite Eq. (17) as follows:

$$\epsilon^*(\omega_E, T, t_a) = \Delta \epsilon \int_0^\infty \tilde{\epsilon}_D^*(\omega_E, \omega) \phi(\omega, T, t_a) g(\omega, T, 0) d(\log_e \omega), \quad (19)$$

where

$$\phi(\omega, T, t_a) \equiv \frac{g(\omega, T, t_a)}{g(\omega, T, 0)}. \quad (20)$$

Here, $\phi(\omega, T, t_a)$ is a relaxation function that describes the change in the distribution function of the α -relaxation rates. As t_a goes to infinity, $g(\omega, \tau, t_a)$ approaches the distribution function of the relaxation rate of the equilibrium state $g(\omega, T, \infty)$. As already mentioned above, $\tilde{\epsilon}'_D(\omega_E, \omega)$ has a peak at $\omega_E = \omega$ and has an appreciable value only for the range between $\omega \xi_D^{-1}$ and $\omega \xi_D$. Here, $\xi_D = 2 + \sqrt{3}$ and $2 \log_{10} \xi_D (= 1.14)$ is the FWHM for the dielectric loss peak of the Debye relaxation. At the same time, $\tilde{\epsilon}'_D(\omega_E, \omega)$ changes from 1 for high relaxation rates to 0 for low relaxation rates over the same range, where $\tilde{\epsilon}''_D(\omega_E, \omega)$ has an appreciable value. In Figs. 7(a) and 7(b), both $\tilde{\epsilon}'_D$ and $\tilde{\epsilon}''_D$ are shown by dotted curves together with the distribution function $g(\equiv g(\omega, T, 0)$ or $g(\omega, T, t_a))$ at a given temperature T_{a1} . Therefore, we can obtain the following approximate equations from Eq. (19):

$$\begin{aligned} \epsilon'(\omega_E, T, t_a) &\approx \Delta \epsilon \int_{\omega_E \xi_D^{-1}}^{\omega_E \xi_D} \tilde{\epsilon}'_D(\omega_E, \omega) \phi(\omega, T, t_a) \\ &\quad \times g(\omega, T, 0) d(\log_e \omega), \end{aligned} \quad (21)$$

$$\begin{aligned} \epsilon''(\omega_E, T, t_a) &\approx \Delta \epsilon \int_{\omega_E \xi_D^{-1}}^{\infty} \tilde{\epsilon}''_D(\omega_E, \omega) \phi(\omega, T, t_a) \\ &\quad \times g(\omega, T, 0) d(\log_e \omega). \end{aligned} \quad (22)$$

The limitation of the integration range in Eqs. (21) and (22) is introduced due to the existence of the factors $\tilde{\epsilon}'_D$ or $\tilde{\epsilon}''_D$ in the integrand. The two factors can be regarded as a filter, through which contributions from the relaxation modes with the relaxation rate $\omega < \omega_E \xi_D^{-1}$ are excluded. In Fig. 7, it is clear why there is such a limitation for the range of the integration. Therefore, if we measure the ac dielectric susceptibility ϵ' (ϵ'') at a given frequency ω_E during aging, we can observe the change in the dynamics and structure of polymer glasses *induced by the modes of the α process with the relaxation rate $\omega > \omega_E \xi_D^{-1}$ ($\omega_E \xi_D^{-1} < \omega < \omega_E \xi_D$)*, although the changes occurs over the entire range of ω .

In order to compare the results given in the previous sections to those of this model, we define the deviation of ϵ' and ϵ'' from the initial value at $t_a = 0$ as follows:

$$\begin{aligned} \Delta \epsilon'(\omega_E, T, t_a) &\equiv \epsilon'(\omega_E, T, 0) - \epsilon'(\omega_E, T, t_a) \\ &= \Delta \epsilon \int_{\omega_E \xi_D^{-1}}^{\infty} \tilde{\epsilon}'_D(\omega_E, \omega) [1 - \phi(\omega, T, t_a)] \\ &\quad \times g(\omega, T, 0) d(\log_e \omega) \end{aligned} \quad (23)$$

and

$$\begin{aligned} \Delta \epsilon''(\omega_E, T, t_a) &\equiv \epsilon''(\omega_E, T, 0) - \epsilon''(\omega_E, T, t_a) \\ &= \Delta \epsilon \int_{\omega_E \xi_D^{-1}}^{\omega_E \xi_D} \tilde{\epsilon}''_D(\omega_E, \omega) [1 - \phi(\omega, T, t_a)] \\ &\quad \times g(\omega, T, 0) d(\log_e \omega). \end{aligned} \quad (24)$$

Here, we consider the effects of temperature change. In this case, the average relaxation rate of the α process, ω_α , changes according to the VFT law and the peak of $g(\omega, T, 0)$ is shifted along the axis of $\log_{10} \omega$, but the shape of $g(\omega, T, 0)$ does not change. This is due to the well-known time-temperature superposition law for the α process, namely, segmental motion in the case of polymeric materials [30]. This can be described by the following scaling law:

$$g(\omega, T, 0) = \tilde{g}\left(\frac{\omega}{\omega_\alpha(T)}\right), \quad (25)$$

where $\tilde{g}(x)$ is a scaled distribution function that satisfies the following relation:

$$\int_0^\infty \tilde{g}(x) d(\log_e x) = 1. \quad (26)$$

In the glassy state, ω_α is located at much lower frequency than the frequency of the applied electric field in our measurement, $f = 20 \text{ Hz} - 1 \text{ MHz}$. As the value ω_α is shifted to a lower value during isothermal aging, g is a decreasing function of aging time t_a at a given value of ω for the range of $\omega > \omega_E \xi_D^{-1}$. This can be verified if the peak of $g(\omega, T, t_a)$ is shifted to a lower frequency side in Fig. 7(a). Therefore, the function $\phi(\omega, T, t_a)$ can also be regarded as the decreasing function of t_a during aging. We here assume that for $\omega > \omega_E \xi_D^{-1}$, $\phi(\omega, T, t_a)$ is independent of ω and can be scaled as follows:

$$\phi(\omega, T, t_a) = \tilde{\phi}(\omega_\alpha(T) t_a), \quad (27)$$

where $\tilde{\phi}(x)$ is a monotonically decreasing function of x . This assumption can be justified as long as the microscopic origin for the change induced during aging is the α process. Using the functions $\tilde{g}(x)$ and $\tilde{\phi}$, Eqs. (23) and (24) can be rewritten as

$$\begin{aligned} \Delta \epsilon'(\omega_E, T, t_a) &\equiv \epsilon'(\omega_E, T, 0) - \epsilon'(\omega_E, T, t_a) \\ &= \Delta \epsilon [1 - \tilde{\phi}(\omega_\alpha(T) t_a)] \int_{\eta_E(T) \xi_D^{-1}}^{\infty} \tilde{\epsilon}'_D\left(\frac{\eta_E(T)}{\eta}\right) \\ &\quad \times \tilde{g}(\eta) d(\log_e \eta) \end{aligned} \quad (28)$$

and

$$\begin{aligned} \Delta \epsilon''(\omega_E, T, t_a) &\equiv \epsilon''(\omega_E, T, 0) - \epsilon''(\omega_E, T, t_a) \\ &= \Delta \epsilon [1 - \tilde{\phi}(\omega_\alpha(T) t_a)] \int_{\eta_E(T) \xi_D^{-1}}^{\eta_E(T) \xi_D} \tilde{\epsilon}''_D\left(\frac{\eta_E(T)}{\eta}\right) \\ &\quad \times \tilde{g}(\eta) d(\log_e \eta), \end{aligned} \quad (29)$$

where $\eta \equiv \frac{\omega}{\omega_\alpha(T)}$ and $\eta_E(T) \equiv \frac{\omega_E}{\omega_\alpha(T)}$.

Now let us consider isothermal aging at $T = T_a$ for t_a hours. After isothermal aging, the value of $\Delta \epsilon'$ ($\Delta \epsilon''$) reaches $\Delta \epsilon'(\omega_E, T_a, t_a)$ ($\Delta \epsilon''(\omega_E, T_a, t_a)$) according to the decay law

given by $\tilde{\phi}(\omega_\alpha(T_a)t_a)$. If we increase the aging temperature T_a for a given frequency ω_E , the relaxation rate $\omega_\alpha(T)$ increases in accordance with the VFT law and hence the factor $1 - \tilde{\phi}(\omega_\alpha(T_a)t_a)$ increases and the value $\eta_E(T_a)$ decreases. Figure 7 shows a schematic picture for the location of g , $\tilde{\epsilon}'_D$, and $\tilde{\epsilon}''_D$ for two different temperatures T_{a1} and T_{a2} ($T_{a1} > T_{a2}$). Only the regions marked by the arrows have significant contributions to the integrals in Eqs. (28) and (29). The area of the region for T_{a1} is clearly larger than that for T_{a2} . Therefore, the values $\Delta\epsilon'$ and $\Delta\epsilon''$ increase with increasing temperature T_a . In this case, we can reproduce the observed aging temperature dependence of the relaxation strength of the ac dielectric susceptibility during isothermal aging. Furthermore, we here consider the case where the frequency of the applied electric field f or ω_E decreases at a given aging temperature T_a . In this case, because η_E decreases with decreasing ω_E , the values $\Delta\epsilon'$ and $\Delta\epsilon''$ increase with decreasing frequency. Therefore, this simple model can qualitatively reproduce the dependence of the relaxation strength $\Delta C''_{\text{total}}$ on the aging temperature and the frequency of the electric field shown in Fig. 4.

Next, we consider the memory and rejuvenation effects observed for the constant-rate mode. We treat the following thermal history. The temperature decreases from a high temperature T_0 to T_{a1} and the temperature is kept at T_{a1} for t_a hours. Then, the temperature decreases from T_{a1} to T_{a2} . After that, the temperature increases again from T_{a2} to T_{a1} , where $T_{a1} > T_{a2}$.

In this case, after isothermal aging at T_{a1} for t_a , $\Delta\epsilon''$ for ω_E will be equal to $\Delta\epsilon''(\omega_E, T_{a1}, t_a)$. We then reduce the temperature from T_{a1} to T_{a2} . The change in aging temperature changes the dynamics of the α process, that is, $\omega_\alpha(T)$ changes from $\omega_\alpha(T_{a1})$ to $\omega_\alpha(T_{a2})$. However, because $T_{a1} > T_{a2}$, it is natural to assume that the structural change induced at a higher temperature does not change after cooling to a lower temperature. In other words, we can assume that the value $\tilde{\phi}(\omega_\alpha(T)t_a)$ does not change for the cooling process, but only the parameter $\eta_E(T)$ changes in accordance with the temperature change. In this case, if the temperature decreases from T_{a1} to T_{a2} at a given frequency ω_E , η_E increases and as a result, $\Delta\epsilon''$ decreases with decreasing temperature. Finally, $\Delta\epsilon''$ vanishes if the temperature T_{a2} is low enough for the divergence of $1/\omega_\alpha(T)$. Therefore, using the present model, we can successfully reproduce the rejuvenation effects observed for ϵ''_{disp} .

During the subsequent heating from T_{a2} to T_{a1} , $\tilde{\phi}(\omega_\alpha(T)t_a)$ does not change, while $\eta_E(T)$ decreases, and hence $\Delta\epsilon''$ increases with increasing temperature. However, above T_{a1} , the structural change induced at T_{a1} may be modified and as a result, $\Delta\epsilon''$ can change abruptly with a further increase in the temperature. Therefore, this model can describe the memory effect with respect to ac dielectric susceptibility. So far, we have discussed only the imaginary part of the complex electrical capacitance ϵ''_{disp} . It is clear that the same argument can be applied to ϵ'_{disp} .

4. Aging of the volume

Now let us consider the volume change, Δv , during isothermal aging. For ac dielectric susceptibility, the existence of $\tilde{\epsilon}'_D$ ($\tilde{\epsilon}''_D$) leads to the limitation of dynamical modes. However, for volume change, *all modes of the α process contribute to the volume change* because the volume is a macroscopic physical quantity. Therefore, we can describe the volume change Δv as follows:

$$\Delta v(T, t) = [1 - \tilde{\phi}(\omega_\alpha(T)t_a)] \int_0^\infty \tilde{g}(\eta) d(\log_e \eta). \quad (30)$$

Here, we adopt the distribution function of the relaxation rate \tilde{g} , which is the same one as for the ac dielectric susceptibility, although the distribution function for Δv may not be the same for ϵ^* . However, what is essential in the present discussion is the fact that there is no ω_E -dependent limitation of the integration range. For isothermal aging at T_a for t_a hours, the total change in volume $\Delta v(T_a, t_a)$ is an increasing function of T_a because the factor $1 - \tilde{\phi}(\omega_\alpha(T)t_a)$ increases with increasing T due to the existence of ω_α .

As for rejuvenation effects, there is no temperature-dependent parameter such as $\eta_E(T)$, in contrast with $\Delta\epsilon'$ and $\Delta\epsilon''$. Only $\tilde{\phi}(\omega_\alpha(T)t_a)$ changes with temperature. However, the structural change induced at T_a is not modified for cooling below T_a . Therefore, we expect that most of the volume change Δv induced at T_a will be retained even at room temperature. In this model, the origin for the different behaviors relating to rejuvenation effects is the existence of the lower bound of the integral $\omega_E(T)$ in the case of the ac dielectric susceptibility. This gives rise to an apparent decrease in the deviation induced during isothermal aging, as the temperature is decreased.

It should be noted that there are many theoretical models that can reproduce interesting aging dynamics in polymeric systems [31]. Some parts of the present model are included in models of physical aging, but what is most important is the introduction of the parameter η_E in the integral of Eqs. (28) and (29). Through this parameter, we can use the same theoretical model to treat the aging behaviors of the ac dielectric susceptibility and the volume.

IV. CONCLUDING REMARKS

In this study, we have measured the capacitance of thin films of P2CS for isothermal aging and for the constant-rate mode:

(1) We have successfully observed the dependence of the ac dielectric susceptibility and the volume on aging temperature and aging time by measuring just the capacitance.

(2) Real and imaginary parts of ac dielectric susceptibility show memory and rejuvenation effects in a similar way as that observed for other polymeric systems such as PMMA and for ac magnetic susceptibility of spin glass.

(3) The volume of glassy states of P2CS does not show full rejuvenation, although it does show a memory effect.

ACKNOWLEDGMENTS

This work was supported by a Grant-in-Aid for Scientific Research (B) (No. 21340121) from the Japan Society for the Promotion of Science and for Scientific Research in the Pri-

ority Area “Soft Matter Physics” from the Ministry of Education, Culture, Sports, Science and Technology, Japan. Finally, the authors would like to express their cordial thanks to the anonymous reviewers for pointing out some errors which existed in the original version of this paper.

-
- [1] J. Mark *et al.*, *Physical Properties of Polymers*, 3rd ed. (Cambridge University Press, London, 2003), Chap. 2.
- [2] G. Strobl, *The Physics of Polymers* (Springer-Verlag, Berlin, 1996).
- [3] L. C. Struick, *Physical Aging in Amorphous Polymers and Other Materials* (Elsevier, New York, 1978).
- [4] A. J. Kovacs, J. J. Aklonis, J. M. Hutchinson, and A. A. Ramos, *J. Polym. Sci., Polym. Phys. Ed.* **17**, 1097 (1979).
- [5] J.-P. Bouchaud, in *Soft and Fragile Matter*, edited by M. E. Cates and M. R. Evans (IOP Publishing, Bristol, 2000), p. 185.
- [6] L. Bellon, S. Ciliberto, and C. Laroche, *Eur. Phys. J. B* **25**, 223 (2002).
- [7] L. Bellon, S. Ciliberto, and C. Laroche, e-print arXiv:cond-mat/9905160.
- [8] K. Fukao and A. Sakamoto, *Phys. Rev. E* **71**, 041803 (2005).
- [9] K. Fukao, A. Sakamoto, Y. Kubota, and Y. Saruyama, *J. Non-Cryst. Solids* **351**, 2678 (2005).
- [10] K. Fukao and S. Yamawaki, *Phys. Rev. E* **76**, 021507 (2007).
- [11] H. Bodiguel, F. Lequeux, and H. Montes, *J. Stat. Mech.: Theory Exp.* 2008, P01020.
- [12] F. Lefloch, J. Hammann, M. Ocio, and E. Vincent, *Europhys. Lett.* **18**, 647 (1992).
- [13] E. Vincent, J.-P. Bouchaud, J. Hamman, and F. Lefloch, *Philos. Mag. B* **71**, 489 (1995).
- [14] K. Jonason, E. Vincent, J. Hammann, J. P. Bouchaud, and P. Nordblad, *Phys. Rev. Lett.* **81**, 3243 (1998).
- [15] K. Jonason, P. Nordblad, E. Vincent, J. Hammann, and J. P. Bouchaud, *Eur. Phys. J. B* **13**, 99 (2000).
- [16] P. Doussineau, T. de Lacerda-Aroso, and A. Levelut, *Europhys. Lett.* **46**, 401 (1999).
- [17] R. L. Leheny and S. R. Nagel, *Phys. Rev. B* **57**, 5154 (1998).
- [18] O. Kircher and R. Böhmer, *Eur. Phys. J. B* **26**, 329 (2002).
- [19] K. Fukao and H. Koizumi, *Eur. Phys. J. Spec. Top.* **141**, 199 (2007).
- [20] K. Fukao and H. Koizumi, *Phys. Rev. E* **77**, 021503 (2008).
- [21] K. Fukao and Y. Miyamoto, *Phys. Rev. E* **61**, 1743 (2000).
- [22] K. Fukao, S. Uno, Y. Miyamoto, A. Hoshino, and H. Miyaji, *Phys. Rev. E* **64**, 051807 (2001).
- [23] R. Greiner and F. R. Schwarzl, *Rheol. Acta* **23**, 378 (1984).
- [24] H. Fröhlich, *Theory of Dielectrics*, 2nd ed. (Clarendon Press, Oxford, 1960), p. 35.
- [25] H. Vogel, *Phys. Z.* **22**, 645 (1921); G. S. Fulcher, *J. Am. Ceram. Soc.* **8**, 789 (1925).
- [26] F. Kremer and A. Schönhals, *Broadband Dielectric Spectroscopy* (Springer, New York, 2003), p. 72.
- [27] K. Fukao, Y. Oda, and D. Tahara (unpublished).
- [28] S. Havriliak and S. Negami, *Polymer* **8**, 161 (1967).
- [29] P. Lunkenheimer, R. Wehn, U. Schneider, and A. Loidl, *Phys. Rev. Lett.* **95**, 055702 (2005).
- [30] N. G. McCrum, B. E. Read, and G. Williams, *Anelastic and Dielectric Effects in Polymeric Solids* (John Wiley & Sons, Ltd., London, 1967), p. 127.
- [31] J. M. Hutchinson, *Prog. Polym. Sci.* **20**, 703 (1995).